Eur. Phys. J. C 9, 557–564 (1999)
DOI 10.1007/s100529900073

THE EUROPEAN PHYSICAL JOURNAL C

CP violation in two-body hadronic decays of B_c mesons*

Youshan Dai[1,2], Dongsheng Du[1]

[1] Institute of High Energy Physics, Chinese Academy of Sciences, P.O. Box 918(4), Beijing, 100039, P.R. China
[2] Department of Physics, Hangzhou University, Hangzhou, 310028, P.R. China

Received: 17 December 1998 / Published online: 30 June 1999

Abstract. Using the next-to-leading-order low-energy effective Hamiltonian, the CP asymmetries for B_c-meson decays into meson pairs are calculated in the spectator approximation. We do not compute the hadronic matrix elements directly; instead, we use the amplitude ratios to estimate the CP asymmetries. This is quite different from previous treatments in the literature. The values of the momentum squared carried by the virtual particles in timelike penguin diagrams are also carefully discussed. From our calculated results, the best decay modes to observe CP violation in B_c decays would be $B_c^- \to \bar{D}^{*0}K^{*-}$, $\bar{D}^0K^{*-}$, $\bar{D}^{*0}K^-$, $\bar{D}^0K^-$, and $B_c^- \to \eta_c D^-$, each of them needs about 10^8 of $B_c^\pm$ events in experiment.

1 Introduction

One of the main aims of B factories is the observation of CP violation. The B_u, B_d, and B_s-meson decays and corresponding CP violation have been discussed extensively. The decays of B_c meson ($\bar{b}c$ and $b\bar{c}$ bound states) provide another valuable window for probing the origin of CP violation. Since a large number of B_c mesons is expected to be produced at hadronic colliders like LHC or Tevatron [1], the examination of the features of B_c-meson decays and CP violation becomes more and more interesting for both experimental efforts and theoretical studies.

Theoretical predictions about B_c-meson decays are made in many previous works using different models [2]. The results are strongly model-dependent. At present, it is difficult to judge these different results, for lack of experimental data. There are also several works which pay attention to CP violation in B_c-meson decays. The Bauer–Stech–Wirbel (BSW) model in [3] and the Bethe–Salpeter formalism in [4] are used to calculate CP-violating asymmetries for two-body mesonic decays of the B_c meson. There are many uncertainties in these calculations, however, due to the model dependence and the different choices of parameter values.

It is well known that only direct CP violation exists in B_c-meson decays, and that it requires that two decay amplitudes have both different weak phases and different strong phases. The weak phases come from the Cabibbo–Kobayashi–Maskawa (CKM) matrix. According to the new experimental results, the favorite values of the Wolfenstein parameters for the CKM matrix are changed; the main difference found when these values are compared with the old ones is the sign of the parameter ρ [5]. Clearly the new Wolfenstein parameter will influence the weak phases as well as the calculated results of the CP-violating asymmetry. If we ignore soft strong phases, which are difficult to estimate at present, hard strong phases can be estimated perturbatively using the low energy effective Hamiltonian and are relevant to the loop-integral functions of penguin diagrams. In general, decay amplitudes and the CP- violating asymmetries rely on hadronic matrix elements, which are strongly model-dependent; but in the spectator approximation (i.e., ignoring the contributions of the annihilation and spacelike penguin diagrams, which are believed to be color- and form-factor-suppressed), CP-violating asymmetries can be obtained without calculation of the hadronic matrix elements for many decay processes of the B_c meson. In this paper, unlike in the previous works in the literature [3,4], we try to estimate the CP-violating asymmetry of the B_c decays into meson pairs without calculating the hadronic matrix elements directly. So that portion of uncertainties caused by the direct computation of the hadronic matrix elements is avoided. Of course, we still need to use factorization approximation to factorize out some coefficients of the decay amplitudes. Thus the factorization approximation will definitely cause its own uncertainties. Another uncertainty source is the unknown momentum squared value carried by the virtual particles in penguin diagrams. In the literature, a special value of k^2 is usually picked up from $[0, m_b^2]$ or $[(1/4)m_b^2, (1/2)m_b^2]$ for all timelike penguin diagrams. This is obviously a rather rough approximation. We shall discuss this problem based on the valence-quark assumption in our paper and try to avoid the drawback of taking arbitrary values for k^2. In this article, we use the next-to-leading-order low-energy effective Hamiltonian [6] to calculate the CP- violating asymmetry for the B_c decays into PP, PV and VV mesons in the spectator approximation (P is a pseudoscalar meson, V a vector meson). In Sect. 2, we

* Supported in part by National Natural Science Foundation of China

first list the formula for the CP-violating asymmetry. The quark-diagram amplitudes using the next-to-leading-order low- energy effective Hamiltonian are given in Sect. 3. In Sect. 4, we discuss the value of k^2 carried by the virtual particles for the timelike penguin diagrams. The calculated results of the CP-violating asymmetries for the B_c decays into meson pairs are given in Sect. 5. Finally, Sect. 6 is devoted to discussion and conclusion.

2 Formula of CP asymmetry

For the B_c-meson decays to a final state f, we may, without loss of generality, write the decay transition amplitude as

$$A(f) = G_1 T_1 + G_2 T_2 \tag{2.1}$$

where G_1, G_2 are both multiplication of the CKM matrix elements. Assuming CPT invariance, the CP-conjugated amplitude is

$$\bar{A}(\bar{f}) = G_1^* T_1 + G_2^* T_2 \tag{2.2}$$

With the help of (2.1) and (2.2), the CP-violating asymmetry can be written as

$$\begin{aligned}\mathcal{A}_{\rm cp}(f) &\equiv \frac{|A(f)|^2 - |\bar{A}(\bar{f})|^2}{|A(f)|^2 + |\bar{A}(\bar{f})|^2} \\ &= \frac{-2({\rm Im}G_1G_2^*)({\rm Im}T_1T_2^*)}{|G_1T_1|^2 + |G_2T_2|^2 + 2({\rm Re}G_1G_2^*)({\rm Re}T_1T_2^*)}\end{aligned} \tag{2.3}$$

Defining $G_1 = |G_1|{\rm e}^{{\rm i}\theta_1}$, $G_2 = |G_2|{\rm e}^{{\rm i}\theta_2}$ and $T_1 = |T_1|{\rm e}^{{\rm i}\delta_1}$, $T_2 = |T_2|{\rm e}^{{\rm i}\delta_2}$, where θ_1, θ_2 are the weak phases and δ_1, δ_2 are the strong phases, respectively, then we have

$$\mathcal{A}_{\rm cp}(f) = \frac{-2\sin(\theta_1-\theta_2)\sin(\delta_1-\delta_2)}{|\frac{G_1T_1}{G_2T_2}| + |\frac{G_2T_2}{G_1T_1}| + 2\cos(\theta_1-\theta_2)\cos(\delta_1-\delta_2)} \tag{2.4}$$

Obviously the decay amplitude must have both different weak phases ($\theta_1 \neq \theta_2$) coming from the CKM matrix, and different strong phases ($\delta_1 \neq \delta_2$) coming from final-state interactions (FSI); otherwise there are no CP violations. We introduce another angle, ζ, which is defined as

$$h \equiv \left|\frac{G_1T_1}{G_2T_2}\right| \equiv tg\frac{\zeta}{2}\,, \qquad \sin\zeta = \frac{2h}{1+h^2} > 0; \tag{2.5}$$

then the CP-violating asymmetry formula becomes

$$\begin{aligned}&\mathcal{A}_{\rm cp}(f) = \mathcal{A}_0/(1+\mathcal{A}_1) \\ &\mathcal{A}_0 = -\sin\zeta\sin(\theta_1-\theta_2)\sin(\delta_1-\delta_2) \\ &\mathcal{A}_1 = \sin\zeta\cos(\theta_1-\theta_2)\cos(\delta_1-\delta_2)\end{aligned} \tag{2.6}$$

We can see that the magnitude of the direct CP violation depends on three angles: the weak phase $(\theta_1-\theta_2)$, the strong phase $(\delta_1-\delta_2)$ and the angle ζ.

(i) The weak phase $(\theta_1-\theta_2)$ is decided by the CKM matrix elements, $\sin(\theta_1-\theta_2) = {\rm Im}G_1G_2^*/|G_1G_2|$, $\cos(\theta_1-\theta_2) = {\rm Re}G_1G_2^*/|G_1G_2|$. According to the Wolfenstein representation of the CKM matrix [7],

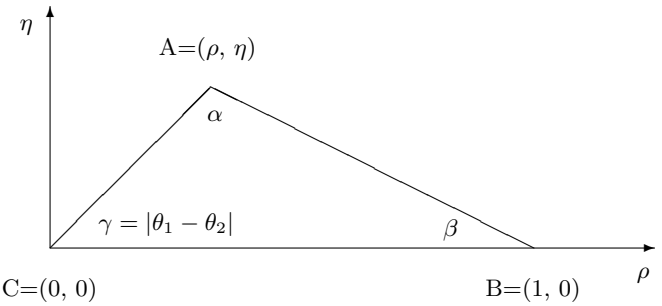

Fig. 1. The unitarity triangle of the CKM matrix elements $V_{ub}^*V_{ud} + V_{cb}^*V_{cd} + V_{tb}^*V_{td} = 0$ in the $(\rho,\,\eta)$ plane

$$\begin{aligned}V &= \begin{pmatrix} V_{ud} & V_{us} & V_{ub} \\ V_{cd} & V_{cs} & V_{cb} \\ V_{tb} & V_{ts} & V_{tb} \end{pmatrix} \\ &= \begin{pmatrix} 1-\frac{\lambda^2}{2} & \lambda & A\lambda^3(\rho-{\rm i}\eta) \\ -\lambda & 1-\frac{\lambda^2}{2} & A\lambda^2 \\ A\lambda^3(1-\rho-{\rm i}\eta) & -A\lambda^2 & 1 \end{pmatrix} + O(\lambda^4)\end{aligned} \tag{2.7}$$

For two-body mesonic B_c^- decays, if we consider only the b quark decay, then we have $|G_1G_2| = |V_{ud}^*V_{cd}^*V_{ub}V_{cb}| = |V_{us}^*V_{cs}^*V_{ub}V_{cb}| \approx A^2\lambda^6(1-\lambda^2/2)\sqrt{\rho^2+\eta^2}$ and ${\rm Im}G_1G_2^* = \pm J \approx \pm A^2\lambda^6(1-\lambda^2/2)\eta$. It follows that

$$\sin(\theta_1-\theta_2) = \pm\frac{\eta}{\sqrt{\rho^2+\eta^2}}\,, \qquad |\theta_1-\theta_2| = \gamma \tag{2.8}$$

where the angle γ is just one of the angles of the unitarity triangle for the CKM matrix elements in Fig. 1. From (2.8), we see that the weak phase $(\theta_1-\theta_2)$ is decided only by the Wolfenstein parameters (ρ,η).

(ii) The strong phase $(\delta_1-\delta_2)$ is caused by final-state interactions, in which the penguin effects (hard strong phases) can be estimated perturbatively, and the rescattering effects (soft strong phases) are unknown at present. In this paper, we will ignore the rescattering effects and discuss the penguin effects only.

(iii) The angle ζ relies on the ratio $h = |G_1T_1/G_2T_2| = tg\zeta/2$. Although the decay amplitudes T_1 and T_2 can both be calculated, there are uncertainties, since the calculation of hadronic matrix elements, T_1, T_2, are model-dependent. However, for many B_c-decay processes, we do not need to compute the decay amplitudes (hadronic matrix elements) individually because the ratio T_1/T_2 is independent of the hadronic matrix elements (in factorization approximation). For example, in our formula of the CP- violating asymmetry, we need only to focus on calculating the ratio h and $\sin\zeta = f(h) = 2h/(1+h^2)$. In the case of $h \ll 1 (or\ h \gg 1)$, we have $\sin\zeta = f(h) \approx 2h$ (or $2/h$) $\ll 1$, $|\mathcal{A}_1| \ll 1$, so the CP-violating asymmetry (2.6) can be simplified as

$$\mathcal{A}_{\rm cp}(f) = \frac{\mathcal{A}_0}{1+\mathcal{A}_1} \approx \mathcal{A}_0 = -\sin\zeta\sin(\theta_1-\theta_2)\sin(\delta_1-\delta_2)$$

$$(\text{for } \ h \ll 1 \ \text{ or } \ h \gg 1) \tag{2.9}$$

3 The quark-diagram amplitudes

Following [6], the next-to-leading-order low-energy effective Hamiltonian for $|\Delta B|$=1 is given at the renormalization scale $\mu \sim m_b$ as

$$\mathcal{H}_{\rm eff}(|\Delta B|=1) = \frac{G_F}{\sqrt{2}} \sum_{\substack{q=u,c \\ q'=d,s}} V_{qq'}V_{qb}^* \{C_1(\mu)Q_1 + C_2(\mu)Q_2 + \sum_{k=3}^{10} C_k(\mu)Q_k\} \ + \ \text{h.c.} \tag{3.1}$$

where the Wilson coefficients $C_i(\mu)$ $(i = 1, 2, \cdots, 10)$ are calculated in the renormalization-group improved perturbation theory and include the leading- and next-to-leading-order QCD corrections. Q_1 and Q_2 are the tree diagram operators, and $Q_3, \cdots, Q_6$ are the QCD-penguin diagram operators, whereas $Q_7, \cdots, Q_{10}$ are the electroweak penguin diagram operators.

$$\begin{aligned}
Q_1 &= (\bar{q'}_\alpha q_\beta)_{V-A}(\bar{q}_\beta b_\alpha)_{V-A} \\
Q_2 &= (\bar{q'}q)_{V-A}(\bar{q}b)_{V-A} \\
Q_{3(5)} &= (\bar{q'}b)_{V-A}\sum_{q''}(\bar{q''}q'')_{V-A(V+A)} \\
Q_{4(6)} &= (\bar{q'}_\alpha b_\beta)_{V-A}\sum_{q''}(\bar{q''}_\beta q''_\alpha)_{V-A(V+A)} \\
Q_{7(9)} &= \frac{3}{2}(\bar{q'}b)_{V-A}\sum_{q''}e_{q''}(\bar{q''}q'')_{V+A(V-A)} \\
Q_{8(10)} &= \frac{3}{2}(\bar{q'}_\alpha b_\beta)_{V-A}\sum_{q''}e_{q''}(\bar{q''}_\beta q''_\alpha)_{V+A(V-A)}
\end{aligned} \tag{3.2}$$

In (3.2), q'' is running over the quark flavors being active at the scale $\mu \sim m_b$ ($q'' \in u, d, s, c, b$), $e_{q''}$ are the corresponding quark charges in unit of $|e|$, α and β are $\mathrm{SU}(3)_c$ color indices, $(V \pm A)$ refer to $\gamma_\mu(1 \pm \gamma_5)$. In general, the nonleptonic B_c decays can occur through both the spectator channels and nonspectator channels. The latter are difficult to deal with at present and are commonly assumed to be form-factor-suppressed, as compared to the former ones. In spectator approximation, the two-body mesonic B_c^- decay can be described by quark diagrams as in Fig. 2. Using $\mathcal{H}_{\rm eff}$ (3.1) in a renormalization-scheme-independent way [8] and factorization approximation, the quark-diagram amplitudes of Fig. 2.(where the CKM matrix elements have been singled out) can be obtained as follows:

$$\begin{aligned}
T(a^{\rm tree}) &= a_1 A, \\
T(a_q^{\rm pen}) &= [(a_3 + a_9) + \xi_f(a_5 + a_7) + (1 + \xi_f)b_1 G_q(k^2)]A, \\
T(b^{\rm tree}) &= a_2 B, \\
T(b_q^{\rm pen}) &= \left[\left(a_3 - \frac{1}{2}a_9\right) + \xi_f\left(a_5 - \frac{1}{2}a_7\right) + (1 + \xi_f)b_2 G_q(k^2)\right]B,
\end{aligned} \tag{3.3}$$

where $T(a^{\rm tree})$ refers to the amplitude of the diagram $a^{\rm tree}$ in Fig. 2, etc., and A and B denote the factorized hadronic matrix elements

$$\begin{aligned}
A &\equiv \tfrac{G}{\sqrt{2}} < X^-|(\bar{q}_1 q_2)_{V-A}|0 >< X^0|(\bar{q}_3 b)_{V-A}|B_c^- > \\
&\quad \text{for } X^- = (q_1\bar{q}_2)\ , \ \ X^0 = (q_3\bar{c}) \\
B &\equiv \tfrac{G}{\sqrt{2}} < X^0|(\bar{q}_1 q_2)_{V-A}|0 >< X^-|(\bar{q}_3 b)_{V-A}|B_c^- > \\
&\quad \text{for } X^0 = (q_1\bar{q}_2)\ , \ \ X^- = (q_3\bar{c})
\end{aligned} \tag{3.4}$$

In (3.3), ξ_f arises from the transformation of $(V-A)(V+A)$ currents into $(S+P)(S-P)$ and then into $(V-A)(V-A)$ ones for Q_{5-8}:

$$\xi_f = \begin{cases} ((1+\eta_{X^-})M_{X^-}^2)/(m_{q'} + m_{q_v})(\eta_{X^0} m_b - m_{q_v}) \\ \quad \text{for } a^{\rm pen} \text{ diagrams} \\ ((1+\eta_{X^0})M_{X^0}^2)/(m_{q'} + m_{q'_v})(\eta_{X^-} m_b - m_{q'_v}) \\ \quad \text{for } b^{\rm pen} \text{ diagrams} \end{cases} \tag{3.5}$$

where

$$\eta_{X^0}\ (\text{or } \eta_{X^-}) = \begin{cases} +1 & for\ X^0 (or\ X^-) = P \\ & \quad (\text{pseudoscalar meson}) \\ -1 & for\ X^0 (or\ X^-) = V \\ & \quad (\text{vector meson}) \end{cases} \tag{3.6}$$

From (3.5) and (3.6), we can see that $\xi_f = 0$ when either X^- is a vector meson in $a^{\rm pen}$ diagrams or X^0 is a vector meson in $b^{\rm pen}$ diagrams. The reason is the following: Using the Fierz rearrangements for Q_{5-8}, the calculated results of the decay amplitudes are proportional to the factor $P^\mu(X^-)\epsilon_\mu(X^-)$ (or $P^\mu(X^0)\epsilon_\mu(X^0)$) which is equal to zero (P^μ and ϵ_μ are the momentum and polarization vectors of the vector meson, respectively). In (3.3), a_k is defined as

$$a_{2i-1} \equiv \frac{\bar{c}_{2i-1}}{N_c} + \bar{c}_{2i}, \quad a_{2i} \equiv \frac{\bar{c}_{2i}}{N_c} + \bar{c}_{2i-1} \quad (i = 1, 2, 3, 4, 5) \tag{3.7}$$

where $\bar{c}_k$ $(k = 1, \cdots, 10)$ are the renormalization-scheme-independent Wilson coefficients $\bar{c}_k(\mu)$ at $\mu \sim m_b$. We use $\alpha_s(m_Z) = 0.118,\ \alpha_{\rm em}(m_Z) = 1/128,\ m_t = 174$ GeV; $\bar{c}_i$ is taken as [9]

$$\begin{aligned}
&\bar{c}_1 = -0.313 \qquad \bar{c}_2 = 1.150 \\
&\bar{c}_3 = 0.017 \qquad \bar{c}_4 = -0.037 \\
&\bar{c}_5 = 0.010 \qquad \bar{c}_6 = -0.047 \\
&\bar{c}_7 = -0.001\alpha_{\rm em} \ \bar{c}_8 = 0.049\alpha_{\rm em} \\
&\bar{c}_9 = -1.321\alpha_{\rm em} \ \bar{c}_{10} = 0.267\alpha_{\rm em}
\end{aligned} \tag{3.8}$$

and

$$\begin{aligned}
b_1 &= 2/3\,[(\alpha_s/8\pi)\bar{c}_2(1 - (1/3N_c)) \\
&\quad + \alpha_{\rm em}/3\pi(\bar{c}_1 + (\bar{c}_2/3))1/N_c] \\
b_2 &= 2/3\,[(\alpha_s/8\pi)\bar{c}_2(1 - (1/3N_c)) \\
&\quad - (\alpha_{\rm em}/6\pi)(\bar{c}_1 + (\bar{c}_2/3))1/N_c]
\end{aligned} \tag{3.9}$$

$$G_q(k^2) = \frac{3}{2}\left[\frac{10}{9} - F_q(k^2)\right] \tag{3.10}$$

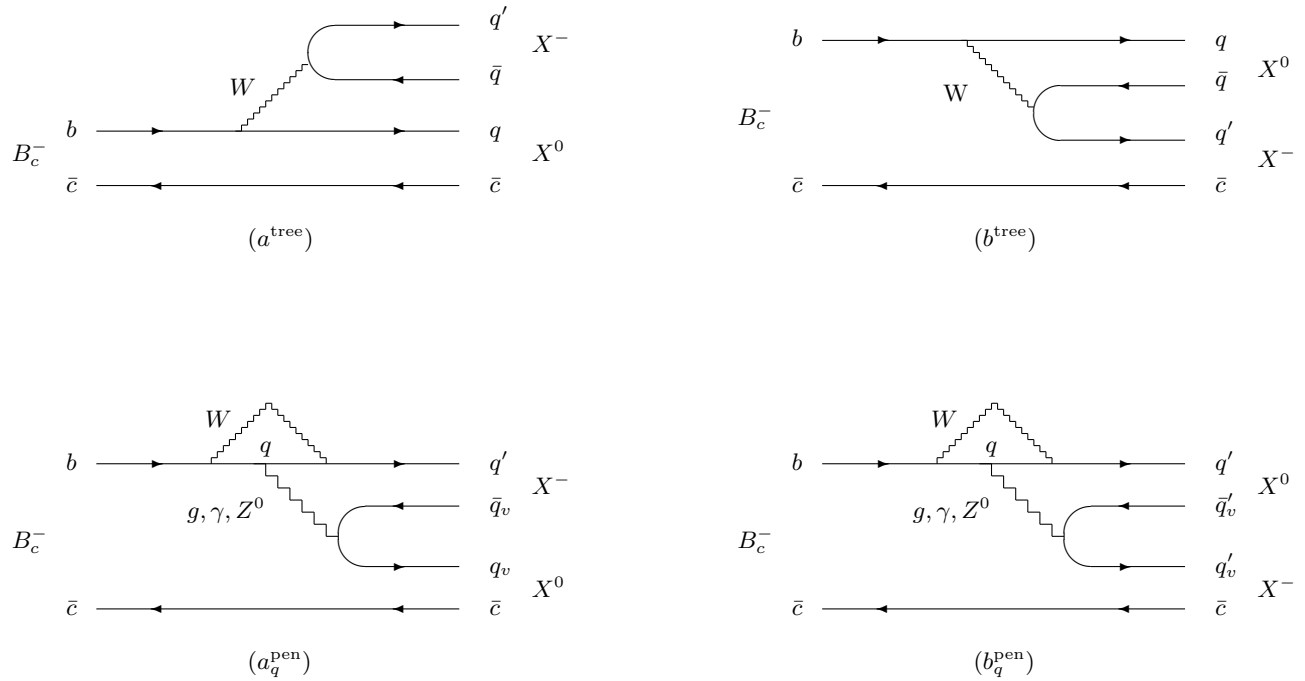

Fig. 2. Quark diagrams for B_c^- decaying into two mesons X^0 and X^- in the spectator approximation. $a^{\rm tree}$ is the color-favored tree diagram; $b^{\rm tree}$ is the color-suppressed tree diagram; $a_q^{\rm pen}$ and $b_q^{\rm pen}$ are the timelike penguin diagrams. Where $q, q_v = u, c$ and $q', q'_v = d, s$; the subscript v denotes "vacuum"

where $F_q(k^2)$ denotes the penguin loop-integral function with momentum transfer squared k^2, at the scale $\mu \sim m_b$,

$$F_q(k^2) = -4\int_0^1 \mathrm{d}x x(1-x)\ln\left[\frac{m_q^2 - x(1-x)k^2}{m_b^2}\right] \quad (3.11)$$

Supposing $k^2 > 4m_q^2$ $(q = u, c)$, and the parameter $r_q = 4m_q^2/k^2 < 1$, the function $G_q(k^2)$ can be analytically expressed as [10]

$$G_q(k^2) = \ln\frac{m_q^2}{m_b^2} - r_q + (1+\frac{r_q}{2})\sqrt{1-r_q}\ln\frac{1+\sqrt{1-r_q}}{1-\sqrt{1-r_q}} + \mathrm{i}\pi(1+\frac{r_q}{2})\sqrt{1-r_q} \quad (3.12)$$

In the case of $q = u$, since $r_u \ll 1$, we have $G_u(k^2) \approx \ln(k^2/m_b^2) + \mathrm{i}\pi$, and the absorptive part of the $G_q(k^2)$ will lead to direct CP violation.

4 The momentum squared carried by the virtual particles

The penguin loop-integral function $F_q(k^2)$ depends crucially on the k^2 carried by the virtual gluon, photon and Z^0. In the literature, a special fixed value of k^2 is usually determined for timelike penguin diagrams from $[0, m_b^2]$ or $[1/4m_b^2, 1/2m_b^2]$ [10], but in general, taking the same value of k^2 for all different quark diagrams is not correct. This problem has been discussed in [11]; we shall discuss it further in the following. For the timelike penguin diagram of

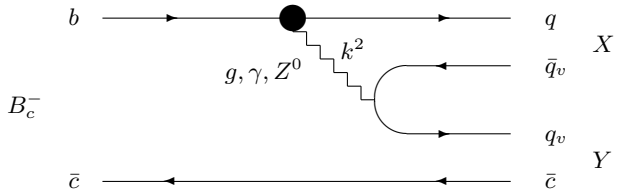

Fig. 3. The timelike penguin diagrams for B_c^- decaying into two mesons X and Y. The dark dot denotes the W loop, the subscript v denotes "vacuum". k^2 is the momentum squared carried by the virtual gluon, photon, and Z^0

the two-body mesonic decay $B_c^- \to \mathrm{XY}$, as illustrated in Fig. 3, we have, using the 4-momentum conservation ($\bar{c}$ as spectator quark),

$$\begin{cases} k^2 = m_b^2 + m_q^2 - 2E_bE_q + 2\mathbf{p_b}\cdot\mathbf{p_q} \\ \mathbf{p_b} = \mathbf{p_q} + \mathbf{p}_{\bar{q}_v} + \mathbf{p}_{q_v} \\ E_b = E_q + E_{\bar{q}_v} + E_{q_v} \end{cases} \quad (4.1)$$

In the rest frame of the X meson, $\mathbf{p_X} = \mathbf{p_q} + \mathbf{p_{\bar{q}_v}} = 0$. Denoting $a \equiv E_q + E_{\bar{q}_v}$, from (4.1), we have

$$\begin{cases} |\mathbf{p_b}| = |\mathbf{p}_{q_v}| \\ E_b = a + E_{q_v}, \end{cases} \qquad \begin{cases} |\mathbf{p_q}| = |\mathbf{p}_{\bar{q}_v}| \\ E_q = a - E_{\bar{q}_v}, \end{cases} \quad (4.2)$$

and we obtain

$$\begin{aligned} E_b &= 1/2a(m_b^2+a^2-m_{q_v}^2)\ , \\ |\mathbf{p_b}| &= 1/2a\sqrt{[(m_b+a)^2-m_{q_v}^2][(m_b-a)^2-m_{q_v}^2]} \\ E_q &= 1/2a(m_q^2+a^2-m_{q_v}^2)\ , \\ |\mathbf{p_q}| &= 1/2a\sqrt{[(m_q+a)^2-m_{q_v}^2][(m_q-a)^2-m_{q_v}^2]}. \end{aligned} \tag{4.3}$$

Because q, $\bar{q}_v$ form a bound state X, in the valence-quark assumption, $p_q = \eta_q p_X + p$ and $p_{\bar{q}_v} = \eta_{\bar{q}_v} p_X - p$, where $\eta_q = m_q/m_q + m_{q_v}, \eta_{\bar{q}_v} = m_{q_v}/m_q + m_{q_v}$; p_X is the total 4-momentum of the bound state X and p is the relative 4-momentum of q vs. $\bar{q}_v$ inside the X meson. In the rest frame of the X meson, it is easy to get $E_q = 1/2M_X(m_q^2 + M_X^2 - m_{q_v}^2)$. So we have $a = M_X$. In (4.1), taking $\mathbf{p_b}\cdot\mathbf{p_q} = |\mathbf{p_b}||\mathbf{p_q}|\cos\varphi$, where φ is the angle between $\mathbf{p_b}$ and $\mathbf{p_q}$ in the rest frame of the X meson, $\varphi = (\mathbf{p_b},\ \mathbf{p_q})$, we get

$$\begin{aligned} k^2(\varphi) &= m_b^2 + m_q^2 - 2E_bE_q + 2|\mathbf{p_b}||\mathbf{p_q}|\cos\varphi, \\ \bar{k^2} &= \frac{1}{\pi}\int_0^\pi \mathrm{d}\varphi k^2(\varphi) = m_b^2 + m_q^2 - 2E_bE_q \end{aligned} \tag{4.4}$$

$$\begin{aligned} (k^2)_{\max} &= m_b^2 + m_q^2 - 2E_bE_q + 2|\mathbf{p_b}||\mathbf{p_q}|\ \ , \\ (k^2)_{\min} &= m_b^2 + m_q^2 - 2E_bE_q - |\mathbf{p_b}||\mathbf{p_q}| \end{aligned} \tag{4.5}$$

where E_b, E_q, $|\mathbf{p_b}|$, $|\mathbf{p_q}|$ can be obtained from (4.3) by taking $a = M_X$. Accordingly we find that the average value of the k^2 is

$$\begin{aligned} \frac{\bar{k^2}}{m_b^2} = \frac{1}{2}\Bigg[1 + \frac{m_{q_v}^2 - m_q^2}{M_X^2}\left(1 - \frac{m_{q_v}^2}{m_b^2}\right) \\ + \frac{m_q^2 + 2m_{q_v}^2 - M_X^2}{m_b^2}\Bigg] \end{aligned} \tag{4.6}$$

For the timelike penguin diagram, $0 \le (k^2)_{\min} \le k^2(\varphi) \le (k^2)_{\max} \le m_b^2$. Since in experiment, φ is unknown, we take the average value of the $\bar{k^2}$ to calculate the penguin loop-integral function. Taking the quark masses m_u, m_d, m_s, m_c, $m_b = 0.005$, 0.01, 0.175, 1.35, 4.8 GeV, respectively, and using the meson masses M_X according to the particle data [12], the values $\bar{k^2}/m_b^2$ of the timelike penguin diagram for different B_c^-- decay processes are given in Table 2.

5 CP asymmetry

As discussed in Sect. 2, the CP-violating asymmetry of B_c-meson decays into meson pairs depends on three angles: the weak phase $(\theta_1 - \theta_2)$, the strong phase $(\delta_1 - \delta_2)$, and the angle ζ. The weak phase $(\theta_1 - \theta_2)$ is determined by the Wolfenstein parameter (ρ, η); the strong phase $(\delta_1 - \delta_2)$ and the angle ζ are decided by the quark-diagram amplitudes. For many decay processes, there is no need to calculate the hadronic matrix elements, because in the factorization approximation, the factorized quark-diagram amplitudes depend only on a single (dominant) hadronic matrix element (A or B), which is canceled in the ratio T_1/T_2.

Below, we discuss as an example the decay process $B_c^- \to \bar{D}^0\pi^-$ to illustrate how to calculate the CP-violating asymmetry in our method. In the spectator approximation, the decay amplitude for the $B_c^- \to \bar{D}^0\pi^-$ is

$$\begin{aligned} A(f) &= G_1T_1 + G_2T_2 \\ &= V_{ud}^*V_{ub}[\ T(a^{\mathrm{tree}}) + T(a_u^{\mathrm{pen}})\ ] + V_{cd}^*V_{cb}T(a_c^{\mathrm{pen}}). \end{aligned} \tag{5.1}$$

Using the quark-diagram amplitude calculated in Sect. 3, we get

$$\begin{aligned} \frac{T_1}{T_2} = \left|\frac{T_1}{T_2}\right| \mathrm{e}^{\mathrm{i}(\delta_1-\delta_2)} = \\ \frac{a_1 + a_3 + a_9 + \xi_{(\bar{D}^0\pi^-)}(a_5+a_7) + [1+\xi_{(\bar{D}^0\pi^-)}]b_1G_u(\bar{k^2})}{a_3 + a_9 + \xi_{(\bar{D}^0\pi^-)}(a_5+a_7) + [1+\xi_{(\bar{D}^0\pi^-)}]b_1G_c(\bar{k^2})} \end{aligned} \tag{5.2}$$

$$\begin{cases} \sin(\delta_1-\delta_2) = \frac{1}{|T_1T_2|}(\mathrm{Im}T_1\mathrm{Re}T_2 - \mathrm{Im}T_2\mathrm{Re}T_1) \\ \cos(\delta_1-\delta_2) = \frac{1}{|T_1T_2|}(\mathrm{Re}T_1\mathrm{Re}T_2 + \mathrm{Im}T_1\mathrm{Im}T_2) \end{cases} \tag{5.3}$$

where $\xi_{(\bar{D}^0\pi^-)} = 2m_{\pi^-}^2/(m_d+m_u)(m_b-m_u) = 0.545$ (for $B_c^- \to \bar{D}^0\pi^-$), $\bar{k^2}/m_b^2 = 0.498, G_u(\bar{k^2}) = -0.697 + \mathrm{i}\pi$, and $G_c(\bar{k^2}) = -2.059 + \mathrm{i}2.500$. Taking $N_c = N_c^{\mathrm{eff}} = 2$, which is favored by experimental data [13], then the numerical results can be obtained as $|T_1/T_2| = 14.55, \sin(\delta_1 - \delta_2) = -0.197, \cos(\delta_1-\delta_2) = -0.980$. From the Wolfenstein representation of the CKM matrix, $G_1 = V_{ud}^*V_{ub} = A\lambda^3(1-\lambda^2/2)(\rho - \mathrm{i}\eta), G_2 = V_{cd}^*V_{cb} = -A\lambda^3$, it follows that

$$\begin{cases} \sin(\theta_1-\theta_2) = \frac{\mathrm{Im}G_1G_2^*}{|G_1G_2|} = \frac{\eta}{\sqrt{\rho^2+\eta^2}} \\ \cos(\theta_1-\theta_2) = \frac{\mathrm{Re}G_1G_2^*}{|G_1G_2|} = \frac{-\rho}{\sqrt{\rho^2+\eta^2}}, \end{cases}$$
$$\begin{cases} h = \left|\frac{G_1T_1}{G_2T_2}\right| = \frac{\lambda^2\sqrt{\rho^2+\eta^2}}{(1-\frac{\lambda^2}{2})}\left|\frac{T_1}{T_2}\right| \\ \sin\zeta = \frac{2h}{1+h^2}. \end{cases} \tag{5.4}$$

According to our CP-asymmetry formula derived in Sect. 2, we have $\mathcal{A}_{\mathrm{cp}} = \mathcal{A}_0/(1+\mathcal{A}_1)$, where $\mathcal{A}_0 = -\sin\zeta\sin(\theta_1 - \theta_2)\sin(\delta_1-\delta_2), \mathcal{A}_1 = \sin\zeta\cos(\theta_1-\theta_2)\cos(\delta_1-\delta_2)$. In this paper, we take $\lambda = 0.220, \eta = 0.336, \rho = 0.160$ (the value of the Wolfenstein parameter A has no effect on our calculation) [5]. For numerical estimation, the results are $\sin(\theta_1-\theta_2) = 0.903, \cos(\theta_1-\theta_2) = -0.430, \sin\zeta = 0.365$ and $\mathcal{A}_0 = 0.0649, \mathcal{A}_1 = 0.154, \mathcal{A}_{\mathrm{cp}}(f = \bar{D}^0\pi^-) = 5.62 \times 10^{-2}$.

The quark-diagram amplitudes for the B_c^- decays into PP, PV, and VV mesons in the spectator approximation are given in Table 1. It can be seen that we need only to compute the ratio T_1/T_2 and that there is no need to calculate the hadronic matrix elements directly in many cases; but for the B_c^--meson decays to $(c\bar{c})D^-, (c\bar{c})D^{*-}, (c\bar{c})D_s^-$,

Table 1. The quark-diagram amplitudes for the B_c^- decays into PP, PV, VV mesons in the spectator approximation

No.	Final state f	The quark-diagram amplitudes
(1)	$\bar{D}^0\pi^-$	
(2)	$\bar{D}^{*0}\pi^-$	$V_{ud}^*V_{ub}[\ T(a^{\rm tree})+T(a_u^{\rm pen})\ ]+V_{cd}^*V_{cb}T(a_c^{\rm pen})$
(3)	$\bar{D}^0\rho^-$	
(4)	$\bar{D}^{*0}\rho^-$	
(5)	π^0D^-	
(6)	π^0D^{*-}	$V_{ud}^*V_{ub}[\ T(b^{\rm tree})+T(b_u^{\rm pen})\ ]+V_{cd}^*V_{cb}T(b_c^{\rm pen})$
(7)	ρ^0D^-	
(8)	ρ^0D^{*-}	
(9)	$K^0D_s^-$	
(10)	$K^0D_s^{*-}$	$V_{ud}^*V_{ub}T(b_u^{\rm pen})+V_{cd}^*V_{cb}T(b_c^{\rm pen})$
(11)	$K^{*0}D_s^-$	
(12)	$K^{*0}D_s^{*-}$	
(13)	η_cD^-	
(14)	ψD^-	$V_{ud}^*V_{ub}T(a_u^{\rm pen})+V_{cd}^*V_{cb}[\ T(a^{\rm tree})+T(b^{\rm tree})+T(a_c^{\rm pen})\ ]$
(15)	η_cD^{*-}	
(16)	ψD^{*-}	
(17)	$\bar{D}^0K^-$	
(18)	$\bar{D}^{*0}K^-$	$V_{us}^*V_{ub}[\ T(a^{\rm tree})+T(a_u^{\rm pen})\ ]+V_{cs}^*V_{cb}T(a_c^{\rm pen})$
(19)	$\bar{D}^0K^{*-}$	
(20)	$\bar{D}^{*0}K^{*-}$	
(21)	$\bar{K}^0D^-$	
(22)	$\bar{K}^0D^{*-}$	
(23)	$\bar{K}^{*0}D^-$	$V_{us}^*V_{ub}T(b_u^{\rm pen})+V_{cs}^*V_{cb}T(b_c^{\rm pen})$
(24)	$\bar{K}^{*0}D^{*-}$	
(25)	ϕD_s^-	
(26)	ϕD_s^{*-}	
(27)	$\eta_cD_S^-$	
(28)	ψD_s^-	$V_{us}^*V_{ub}T(a_u^{\rm pen})+V_{cs}^*V_{cb}[\ T(a^{\rm tree})+T(b^{\rm tree})+T(a_c^{\rm pen})\ ]$
(29)	$\eta_cD_s^{*-}$	
(30)	ψD_s^{*-}	

$(c\bar{c})D_s^{*-}$, the hadronic matrix elements A and B still appear in the ratio

$$\frac{T_1}{T_2}=\frac{a_3+a_9+\xi_f(a_5+a_7)+(1+\xi_f)b_1G_u(\bar{k^2})}{a_1+a_2\frac{B}{A}+a_3+a_9+\xi_f(a_5+a_7)+(1+\xi_f)b_1G_c(\bar{k^2})} \tag{5.5}$$

Fortunately a_2 is color-suppressed compared with a_1, and $B/A\sim O(1)$, so the calculated results are not sensitive to the value of B/A. In this paper, we simply take $B/A=1$ for the estimation of the CP asymmetries of these B_c^--decay processes.

All calculated results of the CP-violating asymmetries for two-body mesonic decays of the B_c^- meson are presented in Table 2.

6 Discussion and conclusion

Using the next-to-leading-order low-energy effective Hamiltonian and the quark-diagram amplitude method, we have calculated the CP-violating asymmetries for two-body mesonic decays of the B_c meson. For most decay processes (except for $B_c^-\to(c\bar{c})D^-$, $(c\bar{c})D^{*-}$, and $(c\bar{c})D_s^-$, $(c\bar{c})D_s^{*-}$), the CP-violating asymmetries do not rely on the hadronic matrix elements, since they are canceled in the ratio T_1/T_2. So there is no model dependence caused by the calculation of the hadronic matrix elements.

The CP-violating asymmetry is proportional to $\mathcal{A}_0=-\sin\zeta\sin(\theta_1-\theta_2)\sin(\delta_1-\delta_2)$. From Table 2, we see that $\sin(\theta_1-\theta_2)$ is the same for all decay processes (except for a sign) which is determined by the Wolfenstein parameters $(\rho,\ \eta)$ only. In the processes (1)–(16), $\sin(\theta_1-\theta_2)=\frac{\eta}{\sqrt{\rho^2+\eta^2}}=0.903, \cos(\theta_1-\theta_2)=\frac{-\rho}{\sqrt{\rho^2+\eta^2}}=-0.430$, and $\left|\frac{G_1}{G_2}\right|=(1-\frac{\lambda^2}{2})\sqrt{\rho^2+\eta^2}$, while in processes (17)–(30),

Table 2. The CP-violating asymmetries for two-body mesonic decays of the B_c^- meson. where $h = |G_1T_1/G_2T_2|$, $\sin\zeta = \frac{2h}{1+h^2}$; $\mathcal{A}_{\rm cp} = \mathcal{A}_0/1 + \mathcal{A}_1$, $\mathcal{A}_0 = -\sin\zeta\sin(\theta_1-\theta_2)\sin(\delta_1-\delta_2)$, $\mathcal{A}_1 = \sin\zeta\cos(\theta_1-\theta_2)\cos(\delta_1-\delta_2)$. In processes (1)–(16), $\sin(\theta_1-\theta_2)$=0.903, $\cos(\theta_1-\theta_2)$=-0.430; while in processes (17)–(30), $\sin(\theta_1-\theta_2)$=-0.903, $\cos(\theta_1-\theta_2)$=0.430

No.	f	ξ_f	$\frac{k^2}{m_b^2}$	$\sin(\delta_1-\delta_2)$	h	$\sin\zeta$	$\mathcal{A}_0$	$\mathcal{A}_1$	$\mathcal{A}_{\rm cp} = \frac{\mathcal{A}_0}{1+\mathcal{A}_1}$	B_r	$\varepsilon_f N$
(1)	$\bar{D}^0\pi^-$	0.545	0.498	-0.197	5.284	0.365	0.0649	0.154	5.62×10^{-2}	2.68×10^{-6}	1.06×10^{9}
(2)	$\bar{D}^{*0}\pi^-$	-0.544	0.498	-0.274	27.93	0.0715	0.0177	0.0296	1.72×10^{-2}	2.18×10^{-6}	1.40×10^{10}
(3)	$\bar{D}^0\rho^-$	0	0.487	-0.202	9.010	0.219	0.0399	0.0922	3.65×10^{-2}	6.85×10^{-6}	9.86×10^{8}
(4)	$\bar{D}^{*0}\rho^-$	0	0.487	-0.202	9.010	0.219	0.0399	0.0922	3.65×10^{-2}	6.81×10^{-6}	9.92×10^{8}
(5)	π^0D^-	0.380	0.500	-0.257	1.462	0.932	0.216	0.387	1.56×10^{-1}	$2.28\times10{-}7$	1.62×10^{9}
(6)	π^0D^{*-}	-0.379	0.500	-0.316	5.528	0.350	0.0999	0.143	8.74×10^{-2}	7.17×10^{-8}	1.64×10^{10}
(7)	ρ^0D^-	0	0.487	-0.255	2.401	0.710	0.163	0.295	1.26×10^{-1}	4.21×10^{-7}	1.35×10^{9}
(8)	ρ^0D^{*-}	0	0.487	-0.255	2.401	0.710	0.163	0.295	1.26×10^{-1}	1.39×10^{-6}	4.08×10^{8}
(9)	$K^0D_s^-$	0.577	0.557	-0.0616	0.3227	0.585	0.0325	-0.251	4.34×10^{-2}	2.38×10^{-7}	2.01×10^{10}
(10)	$K^0D_s^{*-}$	-0.537	0.557	-0.189	0.3066	0.561	0.0957	-0.237	1.25×10^{-1}	2.67×10^{-8}	2.16×10^{10}
(11)	$K^{*0}D_s^-$	0	0.503	-0.0892	0.3161	0.575	0.0463	-0.246	6.14×10^{-2}	1.43×10^{-7}	1.67×10^{10}
(12)	$K^{*0}D_s^{*-}$	0	0.503	-0.0892	0.3161	0.575	0.0463	-0.246	6.14×10^{-2}	2.85×10^{-7}	8.38×10^{9}
(13)	η_cD^-	1.489	0.744	0.261	0.03055	0.0610	-0.0144	0.0253	1.40×10^{-2}	2.95×10^{-4}	1.56×10^{8}
(14)	ψD^-	-0.835	0.744	0.579	0.0007797	0.00156	-0.000816	-0.000547	8.16×10^{-4}	2.19×10^{-5}	6.17×10^{11}
(15)	η_cD^{*-}	0	0.699	0.286	0.01012	0.0202	-0.00522	0.00832	5.18×10^{-3}	6.89×10^{-5}	4.87×10^{9}
(16)	ψD^{*-}	0	0.699	0.286	0.01012	0.0202	-0.00522	0.00832	5.18×10^{-3}	4.95×10^{-4}	6.78×10^{8}
(17)	$\bar{D}^0K^-$	0.565	0.433	-0.173	0.2579	0.484	-0.0756	-0.205	-9.51×10^{-2}	4.67×10^{-6}	2.13×10^{8}
(18)	$\bar{D}^{*0}K^-$	-0.564	0.433	-0.243	1.482	0.927	-0.203	-0.387	-3.31×10^{-1}	4.89×10^{-7}	1.68×10^{8}
(19)	$\bar{D}^0K^{*-}$	0	0.464	-0.194	0.4537	0.753	-0.132	-0.318	-1.94×10^{-1}	3.58×10^{-6}	6.68×10^{7}
(20)	$\bar{D}^{*-}K^{*-}$	0	0.464	-0.194	0.4537	0.753	-0.132	-0.318	-1.94×10^{-1}	3.87×10^{-6}	6.18×10^{7}
(21)	$\bar{K}^0D^-$	0.557	0.434	-0.0975	0.01601	0.0320	-0.00282	0.0137	-2.78×10^{-3}	5.39×10^{-6}	2.16×10^{11}
(22)	$\bar{K}^0D^{*-}$	-0.555	0.434	-0.288	0.01504	0.0301	-0.00783	0.0124	-7.73×10^{-3}	3.05×10^{-7}	4.94×10^{11}
(23)	$\bar{K}^{*0}D^-$	0	0.464	-0.103	0.01593	0.0319	-0.00297	0.0136	-2.93×10^{-3}	3.14×10^{-6}	3.34×10^{11}
(24)	$\bar{K}^{*0}D^{*-}$	0	0.464	-0.103	0.01593	0.0319	-0.00297	0.0136	-2.93×10^{-3}	3.34×10^{-6}	3.14×10^{11}
(25)	ϕD_s^-	0	0.480	-0.0967	0.01599	0.0320	-0.00279	0.0137	-2.75×10^{-3}	1.64×10^{-6}	7.26×10^{11}
(26)	ϕD_s^{*-}	0	0.480	-0.0967	0.01599	0.0320	-0.00279	0.0137	-2.75×10^{-3}	4.23×10^{-6}	2.81×10^{11}
(27)	$\eta_cD_s^-$	1.474	0.708	0.260	0.001549	0.00310	0.000728	-0.00129	7.27×10^{-4}	7.27×10^{-3}	2.34×10^{9}
(28)	ψD_s^-	-0.827	0.708	0.664	0.00003624	0.0000725	0.0000435	0.0000233	4.35×10^{-5}	6.48×10^{-4}	7.34×10^{12}
(29)	$\eta_cD_s^{*-}$	0	0.668	0.285	0.0005167	0.00103	0.000265	-0.000425	2.65×10^{-4}	1.67×10^{-3}	7.67×10^{10}
(30)	ψD_s^{*-}	0	0.668	0.285	0.0005167	0.00103	0.000265	-0.000425	2.65×10^{-4}	1.33×10^{-2}	9.64×10^{9}

$\sin(\theta_1-\theta_2) = -\eta/\sqrt{\rho^2+\eta^2}, \cos(\theta_1-\theta_2) = \rho/\sqrt{\rho^2+\eta^2}$, and $\left|\frac{G_1}{G_2}\right| = \lambda^2\sqrt{\rho^2+\eta^2}/(1-\frac{\lambda^2}{2})$. In processes (1)–(6) and (17)–(20), T_1 is dominated only by the tree diagram and T_2 only by the penguin diagram, so $|T_1| \gg |T_2|$; in processes (9)–(12) and (21)–(26), T_1 and T_2 are both from the penguin diagram contribution only, so $|T_1| \sim |T_2|$; and in the processes (13)–(16) and (27)–(30), T_2 is dominated by the tree diagram and T_1 by the penguin diagram, so $|T_2| \gg |T_1|$. Since the CP-violating asymmetry is proportional to $\sin\zeta = 2h/(1+h^2)$, where $h = |G_1T_1/G_2T_2|$, then if $h \gg 1$ or $h \ll 1$, $\sin\zeta$ is small. From Table 2, The CP-violating asymmetry is suppressed strongly by the small $\sin\zeta$ in the processes $B_c^- \to \psi D^-, \eta_cD_s^-, \psi D_s^-, \eta_cD_s^{*-}, \psi D_s^{*-}$. For the processes with $h \sim O(1)$ ($|G_1T_1| \sim |G_2T_2|$), $\sin\zeta$ is large, such as in the processes $B_c^- \to \pi^0D^-, \rho^0D^-, \rho^0D^{*-}$, $\bar{D}^{*0}K^-, \bar{D}^0K^{*-}, \bar{D}^{*0}K^{*-}$. The hard strong phase $(\delta_1-\delta_2)$ is caused by the interference between penguin and tree diagrams or by penguin diagrams themselves, via the penguin loop-integral functions $G_u(k^2)$ and $G_c(k^2)$. As discussed in Sect. 4, we take the average value of the momentum squared carried by virtual particles for our calculation. In most processes (below the $c\bar{c}$ threshold), $\bar{k^2}/m_b^2 \sim 0.5$, but for producing $c\bar{c}$ pairs $B_c^- \to (c\bar{c})D^-$, $(c\bar{c})D^{*-}$, $(c\bar{c})D_s^-$, and $(c\bar{c})D_s^{*-}$, $\bar{k^2}/m_b^2 \sim 0.7$. From Table 2, we can see that for the processes with interference of penguin diagrams only, such as the processes (9)–(12) and (21)–(26), $|\sin(\delta_1-\delta_2)|$ is smaller than that for the processes with interference between penguin and tree diagrams. So, if the decay satisfy both the conditions that (i) $|G_1T_1| \sim |G_2T_2|$, and (ii) interference occurs between penguin and tree diagrams, then the CP-violating asymmetry will be large, such as that in the processes (5)–(8) and (17)–(20).

According to our CP-violating asymmetry formula $\mathcal{A}_{\rm cp} = \mathcal{A}_{\prime}/\infty + \mathcal{A}_{\infty}$, where $\mathcal{A}_0 = -\sin\zeta\sin(\theta_1-\theta_2)\sin(\delta_1-$

$\delta_2)$, $\mathcal{A}_1 = \sin\zeta\cos(\theta_1-\theta_2)\cos(\delta_1-\delta_2)$, it can be seen that $\mathcal{A}_{\rm cp}$ is proportional to $\mathcal{A}_0$ and that the proportion factor is $1/1+\mathcal{A}_1$. If $|\mathcal{A}_1| \ll 1$, then $\mathcal{A}_{\rm cp} \sim \mathcal{A}_0$. Since $\mathcal{A}_0 \propto \eta$ and $\mathcal{A}_1 \propto \rho$, the CP-violating asymmetry is more sensitive to the parameter η than the parameter ρ. In this paper, we have taken $\rho = 0.160$ [5]; the main difference, as compared with early literature, is a change in the sign of the parameter ρ. For the case of $|\mathcal{A}_1| \ll 1$, the influence of this change is very small, but in the case of $|\mathcal{A}_1| \sim 1$, it is important. In the processes (5)–(8), the CP-violating asymmetry will be smaller than that with minus ρ; while in the processes (17)–(20), it will be larger than that with minus ρ.

In this paper, we do not discuss the decay width of the B_c meson, since the calculation of the hadronic matrix elements are needed, and this is strongly model-dependent. But for testing the CP violation in experiment, we need to find processes with both larger CP-violating asymmetry and larger branching ratios. For the three-standard-deviation (3σ) signature $\varepsilon_f N \sim 9/B_r\mathcal{A}_{\rm cp}^2$, where ε_f is the detecting efficiency of the final state and N is the number of the $B_c^{\pm}$. Since there is a lack of experimental data for the branching fraction of B_c decays at present, in Table 2, we use the results of decay widths for the hadronic decay of the B_c^- calculated in [4], but we take τ_{B_c}=0.5 ps [14] to estimate the branching ratio B_r and $\varepsilon_f N$. This estimation shows that in experiment, the best decay modes to observe CP violation in B_c decays would be $B_c^- \to \bar{D}^{*0}K^{*-}, \bar{D}^0K^{*-}, \bar{D}^{*0}K^-, \bar{D}^0K^-$ and $B_c^- \to \eta_c D^-$, all of which need about 10^8 of $B_c^{\pm}$ events.

In summary, we have calculated the CP-violating asymmetries for the B_c meson decays into PP, PV, VV mesons. This are only relevant to three angles, the weak phase $(\theta_1-\theta_2)$, the strong phase $(\delta_1-\delta_2)$ and the angle ζ. If $|\sin(\delta_1-\delta_2)|$ and $\sin\zeta$ are both large ($|\sin(\theta_1-\theta_2)|$ is the same for all decay processes), the CP- violating asymmetry will be large. There are fewer uncertainties in our calculated CP- violating asymmetries, since we avoided calculating the hadronic matrix elements in our method. In general, we need about 10^8 $B_c^{\pm}$ events for testing the CP violation in experiment.

Finally, we should mention that, in this paper, we have calculated only the hard strong phases; the effects of the soft strong phases would also be important. This needs further study.

Acknowledgements. This work was supported in part by National Natural Science Foundation of China and Beijing Electron Positron Collider National Laboratory.

References

1. J.F. Donoghue, C. Ramirez, G. Valencia, Phys. Rev. D **39**, 1947 (1989); J.F. Donoghue, B.R. Holstein, Phys. Rev. D **40**, 238 (1989); K. Cheung, Phys. Rev. Lett. **71**, 3413 (1993)
2. J. Gasser, H. Leutwyler, Phys. Rep. **87**, 77 (1982); R.D. Peccei, J. Sola, Nucl. Phys. B **281**, 1 (1987); D.S. Du, Z. Wang, Phys. Rev. D **39**, 1342 (1989); J. Bijnens, E. de Rafael, Phys. Lett. B **273**, 483 (1991); J.F. Donoghue, B.R. Holstein, D. Wyler, Phys. Rev. Lett., 3444 (1992); Phys. Rev. D **47**, 2089 (1993); G. Ecker, J. Gasser, Nucl. Phys. B **490**, 239 (1997)
3. M. Masetti, Phys. Lett. B **286**, 160 (1992)
4. J.F. Liu, K.T. Chao, Phys. Rev. D **56**, 4133 (1997)
5. A. Ali, DESY 97-256, [hep-ph/9801270]; F. Parodi, P. Roudeau, A. Slocchi, [hep-ph/9802289]
6. A.J. Buras, M. Jamin, M.E. Lautenbacher, P.H. Weisz, Nucl. Phys. B **400**, 37 (1993) A.J. Buras, M. Jamin, M.E. Lautenbacher, Nucl. Phys. B **444**, 75 (1993); ibid. B **408**, 209 (1993)
7. L. Wolfenstein, Phys. Rev. Lett. **51**, 1945 (1983)
8. A. Buras, M. Jamin, M. Lautenbacher, P. Weisz, Nucl. Phys. B **370**, 69 (1992); ibid. **375**, 501 (1992)
9. N.G. Deshpande, X.G. He, Phys. Lett. B **336**, 471 (1994); Phys. Rev. Lett. **26**, 74 (1995)
10. J.M. Gérard, W.S. Hou, Phys. Rev. Lett. **62**, 855 (1989); Phys. Rev. D **43**, 2909 (1991)
11. D.S. Du, Z.Z. Xing, Phys. Lett. B **349**, 215 (1995)
12. Particle Data Group, Phys. Rev. D **54**, 454 (1996)
13. H.Y. Cheng, B. Tseng, Phys. Rev. D **51**, 6259 (1995)
14. M. Beneke, Fermilab–Pub-95/401-T